Journal of Thermal Analysis and Calorimetry, Vol. 73 (2003) 191–200

DIFFERENTIAL SCANNING CALORIMETRY
An essential tool to characterize $LiMn_2O_4$ spinel

J. M. Amarilla and R. M. Rojas[*]

Instituto de Ciencia de Materiales de Madrid, CSIC, Cantoblanco, 28049 Madrid, Spain

(Received May 24, 2002; in revised form December 5, 2002)

Abstract

A series of $LiMn_2O_4$ samples with nominal Li/Mn molar ratio=1/2 has been synthesized at 700 and 750ºC by the ceramic procedure from Mn_2O_3 and several lithium sources. Lattice parameters determined from X-ray diffraction patterns are within a narrow range, from a_c=8.238(1) Å to a_c=8.245(1) Å, $\Delta a_c/a_c$<0.1%. The study by differential scanning calorimetry (DSC) shows that the temperatures of the cubic (Fd3m)↔orthorhombic (Fddd) phase transition are spread off in a wide range, from –30 to –2ºC for the exothermic C→O phase transition, and from –21 to +13ºC for the endothermic O→C transformation. Relationships between the lattice parameter values, the temperature of the phase transformation, and the stoichiometry of the $LiMn_2O_4$ samples are pointed out. The DSC technique, which reveals more sensitive than X-ray diffraction to very small variations of composition, is put forward as an essential technique to characterize $LiMn_2O_4$ samples.

Keywords: DSC, $LiMn_2O_4$ spinel, phase transformation

Introduction

Lithium-ion or 'rocking-chair' batteries are the state of art of the advanced batteries due to its high potential, elevated energy density, long shelf life and safety [1–3]. $LiMn_2O_4$ spinel is the most promising candidate to substitute $LiCoO_2$ as positive electrode in commercial batteries mainly due to the low cost, and acceptable environmental impact of the manganese compounds [4, 5]. That is the reason why in the last few years the investigations over the lithium manganese spinel based materials have spectacularly stepped up [5–7].

$LiMn_2O_4$ is usually synthesized by the ceramic procedure using mixtures of several manganese and lithium sources heated at temperatures between 600 and 900ºC [8–10]. The samples obtained at about 750ºC show the best electrochemical performance [8]. $LiMn_2O_4$ has been also synthesized by several alternative procedures [11–16]. Electrochemical studies carried out on the so obtained spinels have shown that they present very different electrochemical performances. This result indicates that the electrochemical behavior of the lithium manganese spinels highly depend on the synthesis conditions such

* Author for correspondence: E-mail: rmrojas@icmm.csic.es

1388–6150/2003/ $ 20.00

Akadémiai Kiadó, Budapest
Kluwer Academic Publishers, Dordrecht

as temperature, reagents used as lithium and manganese sources, lithium content, and atmosphere [17–21]. Therefore, to understand the features that control the electrochemical behavior of $LiMn_2O_4$ it is necessary to perform systematic studies about the influence of the synthesis parameters, and to carry out an accurate characterization of the samples. Regarding the latter aspect, the structural characterization of $LiMn_2O_4$ is usually made by X-ray powder diffraction. In addition to the lattice parameter, which is the most usually reported data, this technique also affords information about the purity of the sample. At room temperature, $LiMn_2O_4$ has a spinel type structure with cubic symmetry, space group Fd3m. Yamada *et al.* [22] have shown that on cooling, $LiMn_2O_4$ undergoes a reversible phase transition, which was ascribed to a cubic (Fd3m) to tetragonal ($I4_1/amd$) transformation. Recent Rietveld refinement has shown that the symmetry of the low temperature phase is orthorhombic (Fddd) [23–25]. This structural transformation provokes the appearance in the differential scanning calorimetry (DSC) curve of an exothermic peak for the transition from the high temperature cubic phase to the low temperature orthorhombic phase, and of an endothermic peak for the reverse cubic → orthorhombic transformation [22, 25]. It has also been reported that any subtle deviation of the $LiMn_2O_4$ stoichiometry provokes changes of the average oxidation state of manganese around the theoretical value of 3.5^+, which is reflected on the thermal behavior of the compound [26, 27].

To assess the sensitivity of the DSC technique in the characterization of $LiMn_2O_4$ samples with composition close to the stoichiometric, we have studied a series of $LiMn_2O_4$ spinels with nominal Li/Mn molar ratio=1/2 synthesized at 700 and 750ºC by the ceramic procedure from Mn_2O_3, and different lithium sources. Mn_2O_3 was selected as manganese source because it was shown that the $LiMn_2O_4$ samples synthesized from this reagent had the largest capacity at high current in $Li_4Ti_5O_{12}//LiMn_2O_4$ lithium-ion cells [28]. The temperature, enthalpy and hysteresis width for the C↔O transformation have been determined by differential scanning calorimetry. The relationship among the temperature of the phase transition, the value of the lattice parameter and the composition of the samples has been put forward.

Experimental

$LiMn_2O_4$ samples with molar ratio Li/Mn=1/2 were synthesized by reacting in air at 700 or 750ºC the appropriate amounts of Mn_2O_3 and several lithium salts, i.e. Li_2CO_3, $LiOH{\cdot}H_2O$, and $LiNO_3$. Mn_2O_3 was obtained from thermal decomposition of $MnCO_3$ (Merck) at 700ºC. Li_2CO_3 and $LiNO_3$ were previously dried at 120ºC overnight under dynamic vacuum. The reagents were thoroughly mixed in an agate mortar, fired to 700 or 750ºC for different periods, and then allowed to cool freely in the furnace. The products were carefully grounded again, and then annealed at the synthesis temperature for periods ranging from 24 to 48 h. The samples were labeled **C**, **H** and **N** for $LiMn_2O_4$ obtained from Mn_2O_3 and lithium carbonate, lithium hydroxide or lithium nitrate, respectively. Numbers have been used to differentiate among samples obtained from the same lithium source but submitted to different thermal treatment. Experimental details about the synthesis conditions are summarized in Table 1.

Table 1 Reagents, synthesis conditions, lattice parameter, and temperature, enthalpy and hysteresis width for the cubic↔orthorhombic phase transformation determined from DSC curves of $LiMn_2O_4$ samples

Sample	Reagents	Synthesis conditions	Lattice parameter	[a]Temperature/°C		Enthalpy/mJ mg^{-1}		Hysteresis width/°C
		T/°C/t/h	a_c/Å	exo ($T_{C\rightarrow O}$)	endo ($T_{O\rightarrow C}$)	exo ($T_{C\rightarrow O}$)	endo ($T_{O\rightarrow C}$)	
C	Li_2CO_3+Mn_2O_3	700/120 [b]700/48	8.238(1)	–8.2	+4.8	–7.2	7.2	13
H	$LiOH{\cdot}H_2O$+ Mn_2O_3	700/120 [b]700/48	8.239(1)	–22.1	–11.9	–4.34	4.36	10.2
N1	$LiNO_3$+Mn_2O_3	700/24 [b]700/48	8.2385(8)	–30.3	–21.6	–3.17	3.04	8.7
$\mathbf{N1}_{bis}$	Idem	700/24 [b]700/48	8.2382(6)	–22.6	–15.2	–2.8	3.3	7.4
N2	Idem	700/120 [b]700/48	8.238(1)	–15.2	–5.7	–5.2	5.4	9.5
N3	Idem	750/24 [b]750/24	8.2418(9)	–2.1	+10.4	–6.8	6.8	12.5
N4	Idem	750/24 [b]750/48	8.245(1)	–2.2	+13.1	–8.1	8.1	15.3
$\mathbf{N4}_{800}$	**N4** heated at 800°for 12 h		8.2463(8)	+0.3	+19	–7.6	8.4	18.7
$\mathbf{N4}_{850}$	**N4** heated at 850°for 12 h		8.245(1)	+1.2	+27.3	–7.3	7.7	26.1

[a]measured at the apex of the peaks
[b]annealing

X-ray powder diffraction was performed on a Siemens D-501 (CuK_α) powder diffractometer with monochromatized diffracted beam. Patterns were recorded in the step scanning mode within the range $10 \leq 2\theta \leq 80^o$ with 0.02º (2θ) step scan rate and 3 s counting time. Lattice parameters were refined with the CelRef program [29].

Morphological studies were carried out by scanning electron microscopy on a Zeiss DSC (digital scanning microscope) 960 operating at 100 kV. A drop of the sample dispersed in acetone was leave to dry onto the sample holder, and then coated with gold.

DSC curves were obtained on a Seiko 220U instrument, between –60 and 60ºC. To avoid instrumental effects, analyses were all carried out under strictly identical experimental conditions. The curves were obtained in still air, at 10ºC min^{-1} heating/cooling rates. About ≈25 mg sample was used in each run. Samples were packed by slightly stepping, and situated in open aluminum crucibles. Curves were recorded with and without α-Al_2O_3 as reference material, but no variation in thermal parameters was observed. To check the reproducibility of the experiment, several runs were performed on each sample. Neither shift of the peaks temperature nor variations of the enthalpy were observed from one run to another.

Results

X-ray powder diffraction

X-ray patterns recorded for all the samples could be indexed on a cubic spinel-type cell and lattice parameters are outlined in Table 1. The values are comprised within a narrow range: from a_c=8.238 Å for samples synthesized at 700ºC to a_c=8.245(1) Å for sample **N4** obtained at 750ºC. In Fig. 1a, the patterns of samples **C** and **N1** synthesized at 700ºC from Li_2CO_3 and $LiNO_3$, respectively, are presented.

The effect of the firing temperature was systematically studied on the samples synthesized from Mn_2O_3 and $LiNO_3$. On increasing the reaction temperature from 700 (**N1**) to 750ºC (**N4**), the lattice parameter increases from a_c=8.2385(8) Å to a_c=8.245(1) Å. However, further thermal treatment of the sample **N4** at 800 ($\mathbf{N4}_{800}$) and 850ºC ($\mathbf{N4}_{850}$) does not produce any noticeable variation of the lattice parameter within the experimental error.

Differential scanning calorimetry

DSC curves recorded at 10ºC min^{-1} heating/cooling rate for samples **C** and **N1** are presented in Fig. 1b. This rate was chosen because it provides well-defined peak and reasonable scan time. On cooling from room temperature to –60ºC, DSC curves show an exothermic peak that is ascribed to the cubic to orthorhombic phase transition [25]. In spite of the identical X-ray pattern recorded for these two samples (Fig. 1a), the temperature at the apex of each peak is –8.2 and –30.3ºC for samples **C** and **N1**, respectively. During the heating process, a hysteresis is observed, and the temperatures at the minimum of the corresponding endothermic effect are +4.8 and –21.6ºC for samples **C** and **N1**, respectively. DSC recorded for all others $LiMn_2O_4$ samples synthesized show a similar pattern indicat-

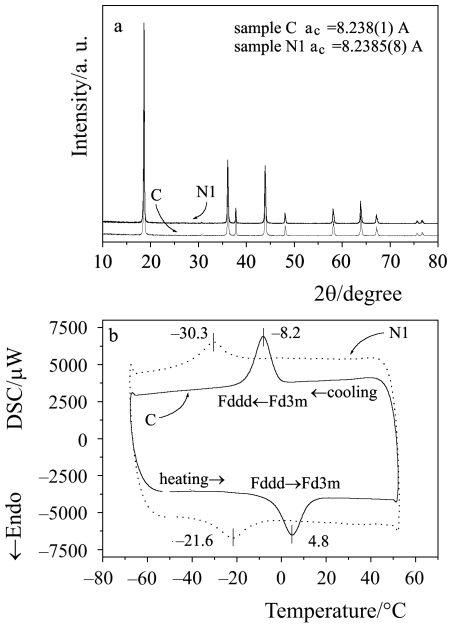

Fig. 1 Plot of: a – X-ray powder diffraction patterns of samples **C** and **N1** synthesized at 700°C from $LiCO_3$ and $LiNO_3$, respectively; b – DSC curves of samples **C** and **N1** recorded at 10°C min^{-1} heating/cooling rate

ing that they undergo similar transformations during the thermal treatment. In Table 1, the temperature at the apex of the exo- and endothermic peaks, the enthalpy, and the hysteresis width determined for each sample have been outlined. It is observed that in spite of the closeness of the lattice parameters, the interval of temperature at which the phase transition takes place is very wide. It ranges from –30.3 (**N1**) to +1.2ºC (**N4**$_{850}$) for the

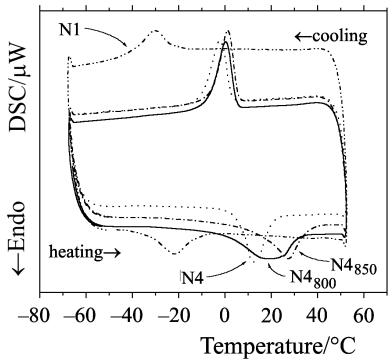

Fig. 2 DSC curves of samples **N1**, **N4**, **N4**$_{800}$, and **N4**$_{850}$ synthesized from $LiNO_3$ at different temperatures. Scan rate 10°C min^{-1}

exothermic C→O transformation, and from –21.6 (**N1**) to +27.3ºC ($\mathbf{N4}_{850}$) for the endothermic O→C transition.

The effect of synthesis temperature on the temperature of the phase transition has been also analyzed on samples prepared from $LiNO_3$. DSC curves obtained for samples **N1**, **N4**, $\mathbf{N4}_{800}$ and $\mathbf{N4}_{850}$ are shown in Fig. 2. It is observed that on increasing the reaction temperature from 700 (**N1**) to 750ºC (**N4**), both the exo- and endothermic peaks significantly shift toward higher temperature. The shift is smaller for the samples annealed at 800 and 850ºC, ($\mathbf{N4}_{800}$ and $\mathbf{N4}_{850}$). The effect of the firing temperature on the temperature of the C↔O phase transition is more evident on the DSC curves recorded on heating from –60ºC.

Scanning electron microscopy

Figure 3 shows the SEM micrographs of a selection of $LiMn_2O_4$ samples. The samples **N1** and **C**, which were obtained at 700ºC, are very homogeneous, with almost identical particle size of ≈0.2 μm (Fig. 3a, b). On increasing the temperature to 750ºC (sample **N4**), the particles become less homogeneous (Fig. 3c). Further heating to 850ºC (sample $\mathbf{N4}_{850}$) causes sintering of the particles, being they of ≈1–2 μm (Fig. 3d).

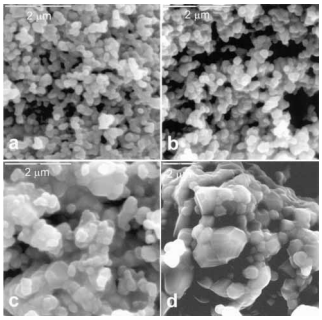

Fig. 3 Scanning Electron Microscopy (SEM) pictures of samples: a – **N1**, b – **C**, c – **N4** and d – $\mathbf{N4}_{850}$

Discussion

X-ray powder diffraction

A series of $LiMn_2O_4$ spinels with nominal Li/Mn molar ratio=1/2 has been obtained as single phases at 700 and 750ºC. The lattice parameters of the samples synthesized at 700ºC are almost identical, a_c≈8.238 Å, independently of what lithium salt was used in the synthesis. The lattice parameters of the samples synthesized at 750ºC are slightly larger, ca. 0.007 Å (≈0.08%). Differences among the lattice parameter of $LiMn_2O_4$ synthesized by different procedures and/or different synthesis conditions have been reported in the literature. Systematic studies carried out on this subject have demonstrated that these differences are due to deviations from stoichiometry [13, 19, 20, 30–33]. Non-

stoichiometry arising either from the lithium excess, $Li_1[Li_xMn_{2-x}]O_4$, or from the occurrence of cation vacancies, $Li_{1-x}[Mn_{2-2x}]O_4$, causes a diminution of the lattice parameter of up to 1%. In both cases, the diminution of the lattice parameter is accounted for by the increase in the Mn^{4+}/Mn^{3+} ratio. On the other hand, oxygen vacancies formed during the thermal treatment of $LiMn_2O_4$ at high temperature increases the a_c value due to the diminution of the Mn^{4+}/Mn^{3+} ratio. The study of the effect of the firing temperature on samples synthesized from $LiNO_3$ has shown that on going from 700 (**N1**) to 750ºC (**N3** and **N4**) the lattice parameter slightly increases, but it remains almost constant after further annealing at 800 and 850ºC. Having in mind that the Li/Mn ratio remains constant throughout the thermal treatment, and that the non-stoichiometry due to oxygen vacancies has been reported for samples heated in inert atmosphere and/or quenched from temperature higher than the ones used in this work [10, 17, 34], the observed increase of the lattice parameter from 700 to 750ºC can be accounted for by the removal of the cation vacancies present in the samples synthesized at 700ºC. This process increases the amount of Mn^{3+}, which ionic radius ($^{VI}Mn^{3+}$= 0.645 Å) is larger than the ionic radius of Mn^{4+} ($^{VI}Mn^{4+}$=0.530 Å) [35] and gives explanation for the increment of lattice parameter observed on increasing the synthesis temperature. A similar evolution with temperature has been described for Nakamura *et al.* [19] for $LiMn_2O_4$ synthesized from several manganese sources, the temperature of the plateau depending on the manganese reagent.

Based on X-ray data it can be concluded that: i) samples synthesized at 700ºC are indistinguishable independently of what lithium salt was used for the synthesis; ii) samples synthesized at 750ºC, with larger lattice parameter are more stoichiometric than the ones synthesized at 700ºC; and iii) the subsequent annealing above 750ºC does not apparently modify the samples.

Differential scanning calorimetry

DSC studies show that the temperatures of the cubic↔orthorhombic phase transition, $T_{C\leftrightarrow O}$, of the samples obtained at 700ºC are very different, being they spread off in a wide interval of ≈25ºC. On increasing the firing temperature, the $T_{C\leftrightarrow O}$ shifts to higher values (Table 1). To investigate the origin of these differences we have analysed the particle size of some selected samples by SEM. Samples **N1** and **C** obtained at 700ºC are very homogeneous and their particle size is almost identical (Fig. 3a, b), but the difference between their phase transition temperatures is of ≈25ºC. In the same way, sample **N4** obtained at 750ºC, with a particle size similar to **N1** (Fig. 3a, c) has a $T_{C\leftrightarrow O}$ ≈30ºC higher. However, sample $\mathbf{N4}_{850}$, with particle size significantly larger, ca. 1–2 μm (Fig. 3d), shows the transition temperatures very close to the $T_{C\leftrightarrow O}$ determined for sample **N4** (Fig. 2). These results allow us to conclude that the differences observed in the $T_{C\leftrightarrow O}$ are not a particle size effect. This conclusion is in agreement with data reported in the literature which show that the effect of the particle size on phase transitions is minimal [36, 37].

The differences in the $T_{C\leftrightarrow O}$ for samples synthesized at 700ºC from different lithium salts can be explained by very small deviations from the theoretical Li/Mn molar ratio=1/2, which are undetectable by chemical analysis. These deviations arise from

hardly-controllable experimental parameters such as lithium salts hydration on weighting, inhomogeneous reaction mixture, etc. It is worth to mention that as the lithium content in $Li_1[Li_xMn_{2-x}]O_4$ increases, the $T_{C\leftrightarrow O}$ decreases progressively, and a lithium excess of only 1.8% (x=0.035) causes a diminution of 60ºC in the $T_{C\leftrightarrow O}$ [26]. Having in mind this result, it can be followed that for the samples synthesized at 700ºC, the lowest the $T_{C\leftrightarrow O,}$ the largest the lithium excess, and hence they would be the less stoichiometric. For the samples synthesized from $LiNO_3$, the increase of the $T_{C\leftrightarrow O}$ on increasing the firing temperatures can be explained by the removal of cation vacancies on heating, giving way to more stoichiometric $LiMn_2O_4$ samples.

The effect of the non-stoichiometry on the $T_{C\leftrightarrow O}$ of the $LiMn_2O_4$ spinels could be accounted for on the basis of the Verwey transition seen in Fe_3O_4 [38, 39]. This transition is explained by the electronic ordering on the Fe^{2+} and Fe^{3+} ions on cooling from room temperature. Recently, Brabers *et al*. [40] have shown that the dope of Fe_3O_4 with divalent and trivalent cations changes the Fe^{2+}/Fe^{3+} ratio on the octahedral sites, disturbs the charge order and provokes the shift of the Verwey transition to lower temperature. In $LiMn_2O_4$, any deviation from stoichiometry causes the Mn^{4+}/Mn^{3+} ratio to deviate from the 1:1 ratio existing in stoichiometric $LiMn_2O_4$. It is plausible to assume that, as in doped Fe_3O_4, this deviation disturbs the partial charge ordering proposed for the orthorhombic $LiMn_2O_4$ [25] and provokes the shift in the $T_{C\leftrightarrow O}$ transition temperature.

The enthalpy and the hysteresis width of the C↔O phase transformation have also been analyzed. In Fig. 4, the plot of the enthalpy and of the hysteresis width *vs*. the temperature for the endothermic O→C transition ($T_{O\rightarrow C}$) is presented. It is observed that the $LiMn_2O_4$ samples with higher transition temperature have also higher enthalpy values, and larger hysteresis width. Having in mind that samples with higher $T_{O\leftrightarrow C}$ are more stoichiometric it can be followed that both the enthalpy and the hysteresis width of the

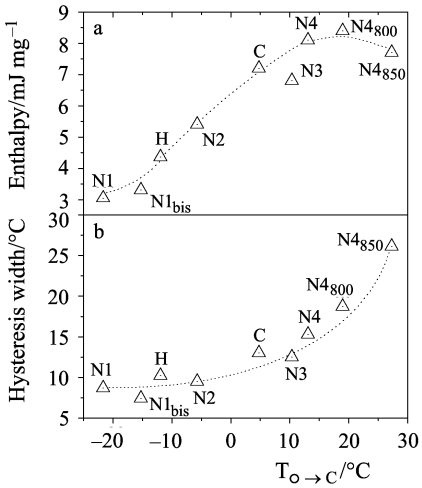

Fig. 4 Plot of a – enthalpy, and b – hysteresis width *vs*. temperature for the endothermic orthorhombic→cubic phase transformation, $T_{O\rightarrow C}$. (Dotted lines are a guide for the eye)

C↔O phase transformation are higher for samples with chemical composition closer to stoichiometric $LiMn_2O_4$. The decrease of enthalpy and the reduction of the hysteresis width can be ascribed to the diminution of the Mn^{4+}/Mn^{3+} partial charge ordering on increasing the non-stoichiometry, and hence to the stabilization of the cubic phase.

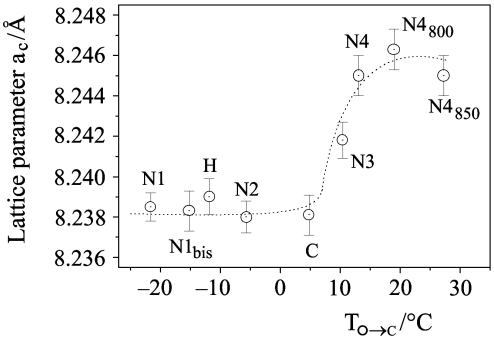

Fig. 5 Lattice parameter *vs.* temperature at the apex of the peak for the endothermic orthorhombic→cubic phase transformation, $T_{O\rightarrow C}$. (The dotted line is a guide for the eye)

Finally, it is worth to compare data afforded by X-ray diffraction and DSC. In Fig. 5 the lattice parameter *vs*. the temperature of the endothermic O→C phase transition ($T_{O\rightarrow C}$) is plotted. The samples with the largest lattice parameter have the highest $T_{C\leftrightarrow O}$ transition, and hence are the most stoichiometric. The likeness among the lattice parameter values for samples synthesized at 700ºC would indicate that these samples could be considered as identical. Nevertheless, the significant differences among the $T_{O\leftrightarrow C}$ determined by DSC clearly show that these samples are different. This sensitivity to very small variations of the stoichiometry makes the DSC technique an essential tool for the characterization of $LiMn_2O_4$ samples.

* * *

The authors deeply acknowledge the financial support of the CICyT (MAT 98-0904) and the Comunidad de Madrid (07N/0072/2002).

References

1 Y. Nishi, in 'Lithium Ion Batteries: Fundamentals and Performance', M. Wakihara, O. Yamamoto Eds Wiley-VCH, Tokyo, Chap. 8 (1998).
2 J. R. Owen, Chem. Soc. Rev., 26 (1997) 259.
3 B. Scrosati, Electrochim. Acta, 45 (2000) 2461.
4 M. Winter, J. O. Beneshad, M. E. Sparth and P. Novák, Adv. Mater., 10 (1998) 725.
5 M. M. Tackeray, Prog. Solid State Chem., 25 (1997) 1.
6 J. M. Paulsen and J. R. Dahn, Chem. Mater., 11 (1999) 3065.
7 X. Sun, H. S. Lee, X. Q. Yang and J. McBreen, Electrochem. Solid State Lett., 4 (2001) A184.
8 V. Manev, B. Banov, A. Momchilov and A. Nassalevska, J. Power Sources, 57 (1995) 99.

9 M. M. Thackeray and M. H. Rossouw, J. Solid State Chem., 113 (1994) 441.
10 Y. Gao and J. R. Dahn, J. Electrochem. Soc., 143 (1996) 100.
11 S. R. S. Prabaharan, M. S. Michael, T. P. Kumar, A. Mani, K. Athinarayanaswamy and R. Gangadharan, J. Mater. Chem., 5 (1995) 1035.
12 W. Liu, G.C. Farrington, F. Chaput and B. Dunn, J. Electrochem. Soc., 143 (1996) 879.
13 V. Massaroti, D. Capsoni, M. Bini, G. Chiodelli, C. B. Azzoni, M. C. Mozzati and A. Paleari, J. Solid State Chem., 147 (1999) 509.
14 W. Yang, X. Huang and L. Chen, J. Power Sources, 81–82 (1999) 647.
15 N. V. Kosova, N. F. Uvanov, E. T. Devyatkina, E. G. Awakumov and S. Y. Solomentsev, Russ. J. Appl. Chem., 73 (2000) 436.
16 W. Yang, G. Zhang, J. Xie, L. Yang and Q. Liu, J. Power Sources, 81–82 (1999) 412.
17 A. Yamada, K. Miura, K. Hinokuma and M. Tanaka, J. Electrochem. Soc., 142 (1995) 2149.
18 Y. K. Sun, K. H. Lee, S. I. Moon and I. H. Oh, Solid State Ionics, 112 (1998) 237.
19 T. Nakamura and A. Kajiyama, Solid State Ionics, 124 (1999) 45.
20 D. S. Ahn and M. Y. Song, J. Electrochem. Soc., 147 (2000) 874.
21 S. Xia, T. Sakai, T. Fujideda, X. Q.Yang, X. Sun, Z. F. Ma, J. Mcbreen and M. Yoshio, J. Electrochem. Soc., 148 (2001) A723.
22 A. Yamada and M. Tanaka, Mat. Res. Bull., 30 (1995) 715.
23 K. Oikawa, T. Kamiyama, F. Izumi, B. C. Chakoumakos, H. Ikuta, M. Wakihara, J. Li and Y. Matsui, Solid State Ionics, 109 (1998) 35.
24 J. Rodríguez-Carvajal, G. Rousse, C. Masquelier and M. Hervieu, Phys. Rev. Lett., 81 (1998) 4660.
25 G. Rousse, C. Masquelier, J. Rodríguez-Carvajal and M. Hervieu, Electrochem. Solid-State Lett., 2 (1999) 6.
26 A. Yamada, J. Solid State Chem., 122 (1996) 160.
27 G. G. Amatucci, C. N. Schmutz, A. Blyr, C. Sigala, A. S. Gozdz, D. Larcher and J. M. Tarascon, J. Power Sources, 69 (1997) 11.
28 J. M. Amarilla, Bol. Soc. Esp. Cerám. Vidrio., 34 (1995) 463.
29 J. Laugier and A. Filhol (CelRef), ILL, Grenoble, France, unpublised, PC version, 1991.
30 R. J. Gummow, A. de Kock and M. M. Tackeray, Solid State Ionics, 69 (1994) 59.
31 Y. Xia and M. Yoshio, J. Power Sources, 57 (1995) 125.
32 C. Masquelier, M. Tabuchi, K. Ado, R. Kanno, Y. Kobayashi, Y. Maki, O. Nakamura and J. B. Goodenough, J. Solid State Chem., 123 (1996) 255.
33 Y. M. Hon, H. Y. Chung, K. Z. Fung and M. H. Hon, J. Solid State Chem., 160 (2001) 368.
34 X. Q. Yang, X. Sun, M. Balasubramanian, J. McBreen, Y. Xia, T. Sakai and M. Yoshio, Electrochem. Solid State Lett., 4 (2001) A117.
35 R. D. Shannon, Acta Crystallogr., A32 (1976) 751.
36 R. C. Mackenzie, in 'Differential Thermal Analysis', Vol. 1, Academic Press, London 1970, p. 108.
37 W. W. Wendlandt, in 'Thermal Methods of Analysis', Wiley 1974, p. 173.
38 E. J. W. Verwey and P. W. Haaymann, Physica, 8 (1941) 979.
39 E. J. W. Verwey, P. W. Haayman and F. C. Romeijn, J. Phys. Chem., 15 (1947) 181.
40 V. A. M. Brabers, F. Walz and H. Kronmüller, Phys. Rev. B, 58 (1998) 163.